



*Citation for published version:*

Nebel, M, Zhang, B, Odoardi, F, Flugel, A, Potter, B & Guse, AH 2015, 'Calcium Signalling Triggered by NAADP in T Cells Determines Cell Shape and Motility During Immune Synapse Formation', *Messenger*, vol. 4, no. 1, pp. 104-111. <https://doi.org/10.1166/msr.2015.1045>

*DOI:*

[10.1166/msr.2015.1045](https://doi.org/10.1166/msr.2015.1045)

*Publication date:*

2015

*Document Version*

Publisher's PDF, also known as Version of record

[Link to publication](#)

As previously, permission has been given by the publisher for this journal for the publishers version to be used

## University of Bath

### General rights

Copyright and moral rights for the publications made accessible in the public portal are retained by the authors and/or other copyright owners and it is a condition of accessing publications that users recognise and abide by the legal requirements associated with these rights.

### Take down policy

If you believe that this document breaches copyright please contact us providing details, and we will remove access to the work immediately and investigate your claim.

AMERICAN  
SCIENTIFIC  
PUBLISHERSCopyright © 2015 American Scientific Publishers  
All rights reserved  
Printed in the United States of America

# Calcium Signalling Triggered by NAADP in T Cells Determines Cell Shape and Motility During Immune Synapse Formation

Merle Nebel<sup>1</sup>, Bo Zhang<sup>3</sup>, Francesca Odoardi<sup>4</sup>, Alexander Flügel<sup>4</sup>,  
Barry V. L. Potter<sup>3</sup>, and Andreas H. Guse<sup>1,2,\*</sup>

<sup>1</sup>The Calcium Signalling Group, Department of Biochemistry and Signal Transduction, University Medical Centre Hamburg-Eppendorf, Martinistrasse 52, 20246 Hamburg, Germany

<sup>2</sup>Department of Biochemistry and Molecular Cell Biology, University Medical Centre Hamburg-Eppendorf, Martinistrasse 52, 20246 Hamburg, Germany

<sup>3</sup>Wolfson Laboratory of Medicinal Chemistry, Department of Pharmacy and Pharmacology, University of Bath, Claverton Down, Bath BA2 7AY, UK

<sup>4</sup>Institute for Multiple Sclerosis Research, Department of Neuroimmunology, Gemeinnützige Hertie-Stiftung and University Medical Centre Göttingen, 37073 Göttingen, Germany

Nicotinic acid adenine dinucleotide phosphate (NAADP) has been implicated as an initial  $\text{Ca}^{2+}$  trigger in T cell  $\text{Ca}^{2+}$  signalling, but its role in formation of the immune synapse in  $\text{CD4}^+$  effector T cells has not been analysed.  $\text{CD4}^+$  T cells are activated by the interaction with peptide-MHCII complexes on the surface of antigen-presenting cells. Establishing a two-cell system including primary rat  $\text{CD4}^+$  T cells specific for myelin basic protein and rat astrocytes enabled us to mirror this activation process *in vitro* and to analyse  $\text{Ca}^{2+}$  signalling, cell shape changes and motility in T cells during formation and maintenance of the immune synapse. After immune synapse formation, T cells showed strong, antigen-dependent increases in free cytosolic calcium concentration ( $[\text{Ca}^{2+}]_i$ ). Analysis of cell shape and motility revealed rounding and immobilization of T cells depending on the amplitude of the  $\text{Ca}^{2+}$  signal. NAADP-antagonist BZ194 effectively blocked  $\text{Ca}^{2+}$  signals in T cells evoked by the interaction with antigen-presenting astrocytes. BZ194 reduced the percentage of T cells showing high  $\text{Ca}^{2+}$  signals thereby supporting the proposed trigger function of NAADP for global  $\text{Ca}^{2+}$  signalling. Taken together, the NAADP signalling pathway is further confirmed as a promising target for specific pharmacological intervention to modulate T cell activation.

**Keywords:** NAADP, T Cell Activation, Cytoskeleton,  $\text{Ca}^{2+}$  Signalling, Live Cell Imaging.

## INTRODUCTION

$\text{Ca}^{2+}$  signalling plays an essential role in early T cell activation. Ligation of the T cell receptor/CD3 complex (TCR/CD3) results in signal transduction across the plasma membrane followed by formation of the second messengers NAADP (Gasser et al., 2006), D-myoinositol 1,4,5-trisphosphate ( $\text{IP}_3$ ; Guse et al., 1995), and cyclic ADP-ribose (cADPR; Guse et al., 1999) in a specific temporal sequence. Among these second messengers, NAADP is unique since it acts at effective concentrations in the nanomolar range (Lee and Aarhus, 1995) and initiates global  $\text{Ca}^{2+}$  signalling as a trigger [reviewed in Guse and Lee (2008)]. Indeed, NAADP is the most potent  $\text{Ca}^{2+}$ -releasing second messenger known so far, present in

mammals, invertebrates and plants [reviewed in Lee, 2012; Morgan et al., 2011].

Though receptor-evoked formation of NAADP has been described in several cell systems (Gasser et al., 2006; Masgrau et al., 2003; Yamasaki et al., 2005; Kim et al., 2008; Barceló-Torns et al., 2011; Lewis et al., 2012) both enzymes involved in NAADP metabolism (Aarhus et al., 1995; Soares et al., 2007; Cosker et al., 2010; Schmid et al., 2011) as well as the NAADP receptor and/or target channel (Mojzisoová et al., 2001; Hohenegger et al., 2002; Gerasimenko et al., 2003, 2006; Dammermann et al., 2009; Zhang and Li, 2007; Zhang et al., 2009; Calcraft et al., 2009; Brailoiu et al., 2009; Ogunbayo et al., 2011; Yamaguchi et al., 2011; Wang et al., 2012) are still a matter of debate. As a unifying hypothesis for NAADP's mode of action, we recently proposed that it might first bind to cytosolic NAADP binding proteins (Lin-Moshier et al., 2012; Walseth et al., 2012); then NAADP bound to

\*Author to whom correspondence should be addressed.

Email: guse@uke.de

its binding protein might activate different channel types, depending on cell type, extracellular stimulus and perhaps other conditions (Guse, 2012).

However, several studies support a trigger function of NAADP for global  $\text{Ca}^{2+}$  signalling. In both pancreatic acinar and islet cells NAADP rapidly increased after stimulation and preceded an increase in cADPR concentration (Yamasaki et al., 2005; Kim et al., 2008). Jurkat T-lymphocytes stimulated via TCR/CD3 show very similar results since NAADP rapidly increased within seconds and likely initiated local  $\text{Ca}^{2+}$  signals in the so-called pacemaker phase of  $\text{Ca}^{2+}$  signalling (Gasser et al., 2006; Kunerth et al., 2004). Infusion or microinjection experiments in Jurkat T cells showed NAADP evoked  $\text{Ca}^{2+}$  signals in restricted trigger zones (Dammermann and Guse, 2005).

While scanning their environment, the cytoskeleton of T cells undergoes permanent changes allowing for both integrin-dependent and -independent types of motion [reviewed in Krummel and Cahalan, 2010]. While integrin-independent motility is more rapid and dependent on myosin, velocity in the integrin-dependent mode is reduced and thus more cell–cell contacts are possible. The situation changes as soon as antigenic peptide in MHCII context is recognized. Then, T cells may either intensify scanning the APC while motility is reduced, but not fully abrogated. Another possibility is formation of the immune synapse (IS) with rounding of T cells and full stop of motility (Donnadieu et al., 1994). The latter is accompanied by ongoing polymerization and inward streaming of actin into the IS (Kaizuka et al., 2007).

Obviously, velocity of T cell motility depends on integrin interactions, but it is less clear what mechanisms underlie the step from intense scanning at low velocity to T cell rounding and full IS formation.  $\text{Ca}^{2+}$  signalling has been implicated in this process and it has been shown that several proteins involved, including proteins involved in  $\text{Ca}^{2+}$  release activated  $\text{Ca}^{2+}$  entry, such as Orai1 and Stim1, or the potassium channels  $\text{K}_{\text{Ca}}3.1$ , and  $\text{K}_{\text{V}}1.3$ , colocalize at the IS [reviewed in (Krummel and Cahalan, 2010)].

In this study we used primary rat MBP-specific T cells and the rat astrocyte cell line F10 (in the following termed “astrocytes”) as APC to analyse the role of NAADP during IS formation. Since we previously demonstrated rapid formation of NAADP, we hypothesized that NAADP mediated local  $\text{Ca}^{2+}$  release might regulate early processes of IS formation, e.g., the step from slowly scanning to immotile rounded T cells. Thus, we recorded in parallel changes in  $[\text{Ca}^{2+}]_i$  cellular shape, and motility of the T cells following contact to astrocytes. The role of NAADP was assessed by blocking NAADP action using the recently validated small-molecule NAADP antagonist BZ194 (Dammermann et al., 2009; Cordiglieri et al., 2010).

## EXPERIMENTAL DETAILS

### Materials

Fura-2/AM was purchased from Calbiochem. DMSO and probenecid were supplied by Sigma. Fibronectin was obtained from Invitrogen. BZ194 was synthesized as described (Dammermann et al., 2009).

### Antigens

Antigen specific T cell clones were specific for guinea pig myelin basic protein (MBP). MBP was purified from guinea pig brains as reported (Eylar et al., 1979).

### Generation and Culturing of T Cells

Rat antigen-specific T cell clones were obtained from lymph node preparations of Lewis rats immunized with MBP. Stimulation, expansion and culture of specific rat T cells were conducted under conditions as described (Flügel et al., 1999).

### Analysis of $[\text{Ca}^{2+}]_i$ , Shape and Motility

Rat  $T_{\text{MBP}}$  cells were loaded with Fura-2/AM as described (Guse et al., 1993) and kept in the dark at  $\sim 15^\circ\text{C}$  until use. Rat F10 astrocytes with up-regulated MHC II (after 48 h-incubation with T cell-blast-conditioned medium) were cultured on  $\mu$ -slides 8 well (ibidi, Martinsried, Germany) on fibronectin and pulsed or not with MBP (10  $\mu\text{g}/\text{ml}$ , 2 hours). Ratiometric  $\text{Ca}^{2+}$  imaging was performed as described recently (Berg et al., 2000). We used an Improvion imaging system (Tübingen, Germany) built around the Leica microscope at 40-fold magnification. Illumination at 340 and 380 nm was carried out using a monochromator system (Polychromator IV, TILL Photonics, Gräfelfing, Germany). Images were taken with a grayscale CCD camera (type C4742-95-12ER; Hamamatsu, Enfield, United Kingdom) operated in 8-bit mode. The spatial resolution was  $510 \times 672$  pixels. The acquisition rate was  $\sim 1$  ratio in 10 seconds. Raw data images were stored on a hard disk. The images were used to construct ratio images (340/380). Finally, ratio values were converted to  $\text{Ca}^{2+}$  concentrations by external calibration. To reduce noise, ratio images were subjected to median filter ( $3 \times 3$ ) as described previously.<sup>42</sup> Data processing was performed using Openlab software (Improvion, Tübingen, Germany). Image J software (freeware, provided by Wayne Rasband, NIH) was used to evaluate cell shape and velocity. Shape index is defined as  $P^2/4\pi S$  (P: perimeter; S: surface of the cell; Donnadieu et al., 1994).

## RESULTS

Fura2-loaded  $T_{\text{MBP}}$  cells were added to a monolayer of astrocytes and fluorescence images were used to monitor

[Ca<sup>2+</sup>]<sub>i</sub> of the T cells. For every tenth fluorescence image a transmitted light image was obtained to follow the interaction of T cells with astrocytes. Time-point zero is defined as first visible contact between a T cell and an astrocyte, as assessed by bright field microscopy.

In the absence of the specific antigen, the T<sub>MBP</sub> cells remained predominantly quiescent without much alteration of [Ca<sup>2+</sup>]<sub>i</sub> (Fig. 1(A), images and upper panel). Within the first ten minutes after contact to the astrocytes, we defined high- and low-responder T cells showing an increase in [Ca<sup>2+</sup>]<sub>i</sub> ≥ 300 nM (high-responder) or < 300 nM (low-responder). Over 90% of the T cells stayed below a [Ca<sup>2+</sup>]<sub>i</sub> of 300 nM in the absence of MBP (Fig. 1(A), images and upper panel). Although T cells added to astrocytes were more or less spherical, their shape changed constantly during the experiment. Several pseudopodia reached out indicating a continuous search for specific antigen. This process was quantitatively analysed using the shape index, where an ideal circular shape corresponds to a shape index of 1 and any deviation increases this value (Fig. 1(A)

middle panel (Donnadieu et al., 1994); for details see Methods Section). In addition, T cells were still mobile and tended to move around rather than staying in contact with one astrocyte (Fig. 1(A) lower panel). In contrast, when T<sub>MBP</sub> cells recognized MBP-pulsed astrocytes, within tens of seconds the majority of the T<sub>MBP</sub> cells displayed high [Ca<sup>2+</sup>]<sub>i</sub> responses (Fig. 1(B), images and upper panel). These high-responder T<sub>MBP</sub> cells started to round up immediately after onset of the Ca<sup>2+</sup>-signal (Fig. 1(B), middle panel) and showed strong immobilization (Fig. 1(B), lower panel). Immobilization led to a stable interaction with astrocytes for the duration of the measurement indicating full formation of IS.

Although cellular characteristics such as shape and motility are individual parameters with quite high differences between individual T cells, grouping the T cells into high- and low-responders in terms of Ca<sup>2+</sup> signalling and averaging the single cell data revealed marked differences between the two groups (Fig. 2). In the absence of MBP 10 out of 12 T<sub>MBP</sub> cells showed an increase in

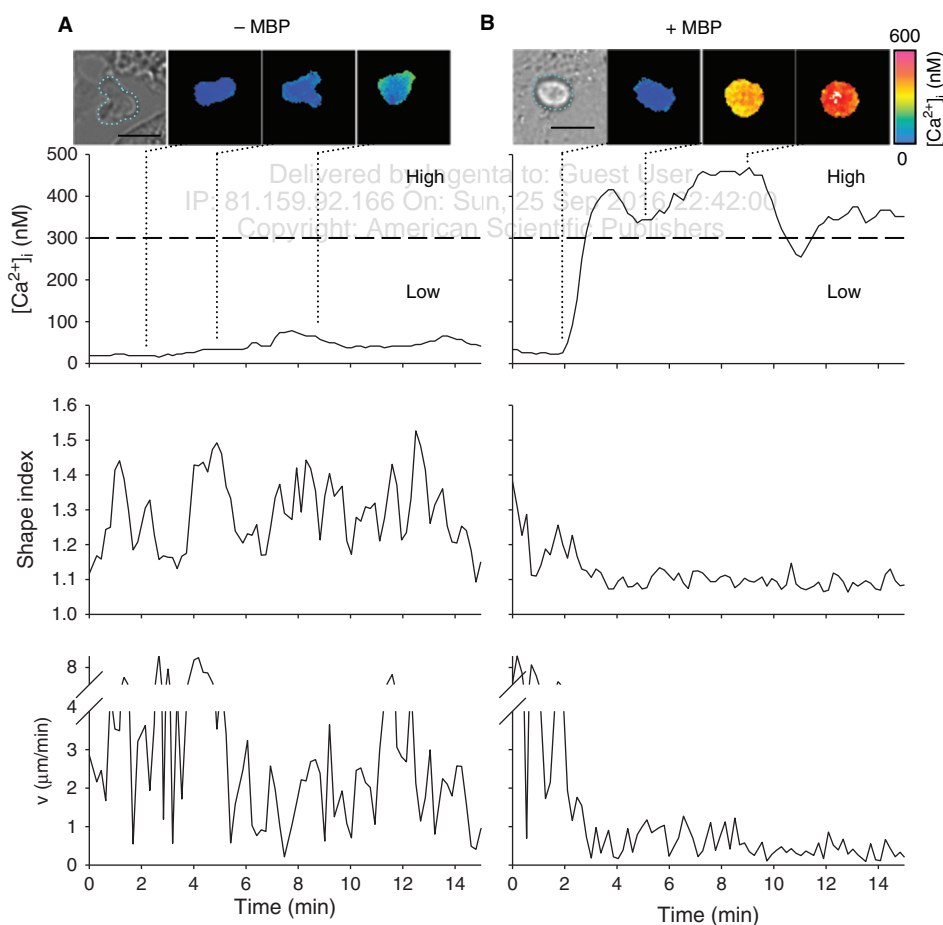


**Figure 1.** Ca<sup>2+</sup> signalling, shape index and motility of T<sub>MBP</sub> cells during immune synapse formation. Astrocytes were pulsed (A) or not (B) with MBP. Resting rat T<sub>MBP</sub> cells were added to the astrocytes and Ca<sup>2+</sup>-signalling, shape index and motility were analysed. Top: Transmitted light and colour-coded images showing single cell analyses of representative T cells. T cells are highlighted by green lines in the transmitted light images. Length scale = 10 µm. Quantification of [Ca<sup>2+</sup>]<sub>i</sub>, changes in shape index and motility in the first 15 minutes after contact to an astrocyte are shown in the panels below.

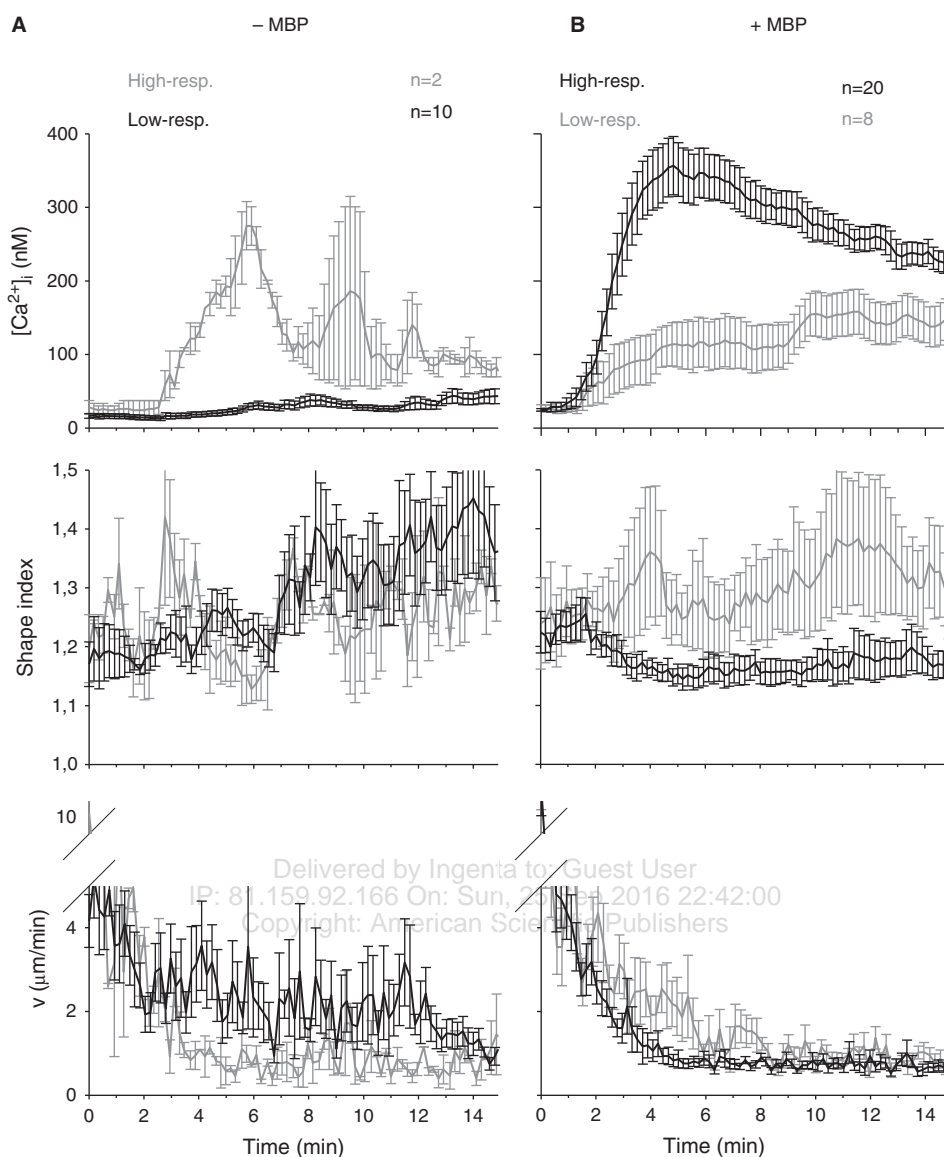


**Figure 2.**  $\text{Ca}^{2+}$  signalling, shape and motility pattern of high- and low-responding  $T_{\text{MBP}}$  cells. Mean  $[\text{Ca}^{2+}]_i$ , shape index and motility of  $T_{\text{MBP}}$  cells after contact to MBP-pulsed (right) astrocytes are displayed ( $\pm$ SEM). Control T cells with non-pulsed astrocytes are shown on the left. Black lines correspond to the majority and grey lines to the minority of T cells at a certain condition (+/- MBP).

$[\text{Ca}^{2+}]_i < 300$  nM in the first ten minutes. This majority of cells, the typical low-responder  $T_{\text{MBP}}$  cells, were low in  $[\text{Ca}^{2+}]_i$  (Fig. 2(A), upper panel), displayed an increased shape index over time (Fig. 2(A), middle panel), and showed motilities between 2 and 3  $\mu\text{m}/\text{min}$  on average (Fig. 2(A), lower panel). Upon presentation of MBP by the astrocytes, the typical high-responder  $T_{\text{MBP}}$  cells were in the majority (Fig. 2(B), upper panel). Further, cellular rounding as judged by a drop in cell shape upon IS formation was observed (Fig. 2(B), middle panel). The  $T_{\text{MBP}}$  cells were virtually “caught” by the astrocytes since also the motility decreased in parallel to cellular rounding (Fig. 2(B), lower panel). Although, low-responders in the presence of antigen started to immobilize, too, this arrest was not as strong as for the high-responders.

Having this cellular assay with three read-outs at hand, the role of NAADP in formation of the IS was analysed. Recently, we showed that the small molecular NAADP antagonist BZ194 blocks local and global  $\text{Ca}^{2+}$  signalling evoked by NAADP, but not by cADPR,  $\text{IP}_3$  or by activation of capacitative  $\text{Ca}^{2+}$  entry evoked by thapsigargin (Dammermann et al., 2009). Here, we demonstrate that BZ194 decreases the overall  $\text{Ca}^{2+}$ -response of  $T_{\text{MBP}}$  cells by reducing the percentage of high-responder cells (Fig. 3, pie diagrams and upper panel). Upon preincubation with BZ194, 56% of the T cells showed a low  $\text{Ca}^{2+}$  response after contact to MBP peptide-presenting astrocytes, whereas in vehicle controls only 30% of T cells were low-responders (Fig. 3, pie diagrams). In this series of experiments, without antigen none of the T cells showed an



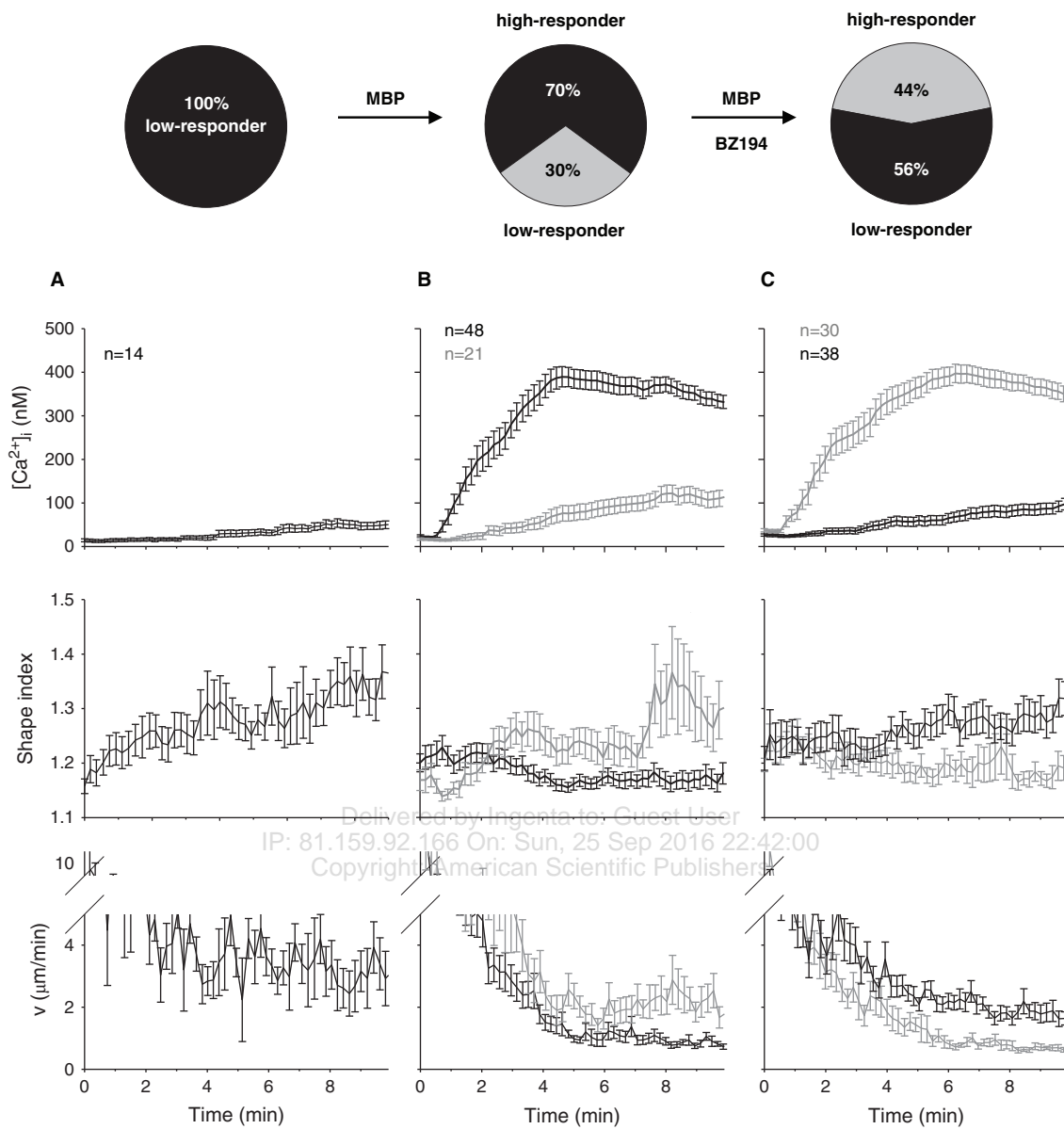


**Figure 3.** NAADP-antagonist BZ194 inhibits  $\text{Ca}^{2+}$ -signalling and immune synapse formation in  $T_{\text{MBP}}$  cells stimulated by MBP-pulsed astrocytes. Astrocytes were pulsed with MBP. Resting rat  $T_{\text{MBP}}$  cells were incubated with BZ194 (C) or left untreated (B). In control experiments astrocytes were not pulsed with MBP (A). T cells were added to the astrocytes and  $\text{Ca}^{2+}$ -signalling was measured. Top: Percentage of T cells showing  $\text{Ca}^{2+}$ -signals above (high-responders) or below (low-responders) 300 nM  $[\text{Ca}^{2+}]_i$  in the first ten minutes after contact to an astrocyte. Bottom: Averaged tracings ( $\pm$ SEM) of T cells showing kinetics of  $[\text{Ca}^{2+}]_i$ , changes in shape index and motility in the first ten minutes after contact to an astrocyte. The majority of T cells is displayed in black, the minority in grey.

increase in  $[\text{Ca}^{2+}]_i > 300$  nM in the first ten minutes after contact (Fig. 3, pie diagrams and A, upper panel). Although BZ194 shifted the percentage of high-responders from 70% down to 44% (Fig. 3, pie diagrams), it is important to note that there was no further influence of BZ194 on the extent of immobilization and rounding up in BZ194 treated high responder  $T_{\text{MBP}}$  cells. Typically,  $T_{\text{MBP}}$  cells showed stronger immobilization and rounding up the higher  $[\text{Ca}^{2+}]_i$  rose (Fig. 3(B)). The same was observed for  $T_{\text{MBP}}$  cells pre-incubated with BZ194 (Fig. 3(C)). Although less of these  $T_{\text{MBP}}$  cells showed high  $\text{Ca}^{2+}$  responses in the presence

of MBP, they were neither impaired regarding their shape change nor in motility. These high-responder  $T_{\text{MBP}}$  cells, though diminished in number, were still capable to round up and slow down to approx. 1  $\mu\text{m}/\text{min}$  during  $\text{Ca}^{2+}$  signalling (Fig. 3(C)). In contrast, the majority of BZ194-treated low-responding  $T_{\text{MBP}}$  cells extended several pseudopodia and moved around on top of the astrocyte layer (Fig. 3(C)). This indicates that BZ194 is able to block  $\text{Ca}^{2+}$  signalling without affecting other essential cellular processes like shape changes due to cytoskeletal rearrangements and motility.

## DISCUSSION

Upon IS formation between CD4+ T<sub>MBP</sub> cells and astrocytes we observed (i) rapid T cell Ca<sup>2+</sup> signalling, and (ii) concomitant decrease in cell shape index (rounding) and motility. While the percentage of high-responder T<sub>MBP</sub> cells increased from very few in the absence to about 70% in the presence of antigenic peptide, inhibition of NAADP signalling reduced the percentage down to 44%, thereby partially reverting antigenic stimulation.

Several aspects of the NAADP signalling pathway have been analysed in T cells. In the CD4+ T-lymphoma cell line Jurkat, TCR/CD3 ligation evoked a biphasic increase in NAADP, consisting of a rapid and high rise within the first 10 to 20 sec followed by a much smaller and slower increase over the next minutes (Gasser et al., 2006). Upon microinjection into Jurkat T cells, NAADP stimulated Ca<sup>2+</sup> signalling with a bell-shaped concentration-response curve (Berg et al., 2000). Both initial local as well as global Ca<sup>2+</sup> signals observed upon NAADP administration were sensitive to gene silencing of ryanodine receptors (Langhorst et al., 2004; Dammermann and Guse, 2005). Unexpectedly, evidence for involvement of acidic Ca<sup>2+</sup> stores in NAADP signalling was not obtained in CD4+ Jurkat T cells,<sup>45</sup> though a recent paper reported Ca<sup>2+</sup> release from acidic cytolitic granules of CD8+ T cells (Davis et al., 2012). In rat CD4+ effector T cells NAADP signalling turned out to be a major player in the cellular activation process, likely by delivering trigger Ca<sup>2+</sup> that acts as co-agonist at IP<sub>3</sub>R and RyR (Dammermann et al., 2009). This finding was confirmed in a transfer experimental autoimmune encephalomyelitis (EAE) rat model, often used to mimic aspects of the human disease multiple sclerosis. Cordiglieri et al., showed that treatment of rats with NAADP antagonist BZ194 interfered with movements of effector T cells towards the central nervous system and decreased re-activation of MBP specific CD4+ effector T cells in the brain (Cordiglieri et al., 2010). Importantly, several control experiments in whole animals or rat T cells indicate no obvious side effects of BZ194 suggesting sufficient specificity of the antagonist. Taken, together NAADP signalling plays a pivotal role for activation of CD4+ T cells. Rapid formation of endogenous NAADP and immediate local Ca<sup>2+</sup> signalling upon NAADP microinjection are compatible with the idea that NAADP provides the first increase in [Ca<sup>2+</sup>]<sub>i</sub> that is used then to enhance CICR via IP<sub>3</sub>R and RyR.

IS formation occurred as soon as [Ca<sup>2+</sup>]<sub>i</sub> increased, visible as rapid cellular rounding and the stop of cell motility in our experiments, as demonstrated in Donnadieu et al. (1994). Reorganization of the actin cytoskeleton is a hallmark of IS formation. Signalling proteins involved in this process are the Rho family GTPases Rac1 and Cdc42, and downstream of Cdc42 the Wiskott-Aldrich syndrome protein WASp (Badour et al., 2003). Moreover, downstream of Rac1 WAVE2 and WAVE2 complex proteins,

such as Abi-2 and HEM-1, appear important for actin reorganization since WAVE2 co-localized to IS (Nolz et al., 2006). Furthermore, gene silencing of WAVE2 and HEM-1 reduced the number of cell–cell conjugate formation (Nolz et al., 2006). Moreover, it was demonstrated that under control conditions, Jurkat T cells formed a ring-like lamellipodal interface composed of F-actin on OKT3-coated surface within 1.5 min; upon gene silencing of WAVE2, these ring-like lamellipodal interfaces were not observed resulting in lack of spreading of T cells on the OKT3-coated surface (Nolz et al., 2006). Kaizuka et al., elegantly tracked movements of TCR, ICAM-1 and actin filaments during the process of IS formation (Kaizuka et al., 2007). Importantly, they showed that in IS-forming Jurkat T cells actin speckles moved from peripheral lamella towards the IS in a directed fashion, forming a ring of actin filaments around the central supramolecular activation cluster (cSMAC). Under these conditions, the retrograde flow of actin typical for moving cells was stopped. Instead, T cells used the actin cytoskeleton for cSMAC and peripheral supramolecular activation cluster (pSMAC) formation. Microclusters composed of TCR and ICAM-1 move along underlying cytoskeleton towards the synapse to form cSMAC and pSMAC, though at slower velocity.<sup>37</sup> This shift of actin cytoskeleton action was determined as decreasing cell shape index in our experiments. Since in our experiments NAADP antagonist BZ194 prevented cell rounding and stop of motility, NAADP mediated initiation of Ca<sup>2+</sup> signalling appears a central step in remodelling of the actin cytoskeleton. Although ring-like lamellipodal interfaces were formed rapidly after TCR/CD3 engagement (within 1.5 min; Nolz et al., 2006), we described an even faster biochemical signalling event, the formation of NAADP within 10 to 20 sec upon anti-CD3 mAb stimulation (Gasser et al., 2006). Based on our experimental data, we cannot distinguish whether NAADP evoked, and initially localized Ca<sup>2+</sup> release would be sufficient to shift actin cytoskeletal function from motility to IS formation, or whether NAADP evoked Ca<sup>2+</sup> release is simply necessary to provide a sufficiently high Ca<sup>2+</sup> signal via IP<sub>3</sub>R and/or RyR to induce the shift in actin cytoskeletal function. However, our data indicate a pivotal role of NAADP signalling for IS formation and thus for activation of CD4+ T cells in general.

## Abbreviations

APC	antigen presenting cell
[Ca <sup>2+</sup> ] <sub>i</sub>	free cytosolic Ca <sup>2+</sup> concentration
cADPR	cyclic ADP-ribose
CICR	Ca <sup>2+</sup> -induced Ca <sup>2+</sup> -release
c(p)SMAC	central (peripheral) supramolecular activation cluster
IP <sub>3</sub>	D- <i>myo</i> -inositol 1,4,5-trisphosphate
IP <sub>3</sub> R	D- <i>myo</i> -inositol 1,4,5-trisphosphate receptor

IS	immune synapse
MBP	myelin basic protein
NAADP	nicotinic acid adenine dinucleotide phosphate
TCR/CD3	T cell receptor/CD3-complex
T <sub>MBP</sub>	cells, MBP-specific T cells.

**Acknowledgments:** This work was supported by the Deutsche Forschungsgemeinschaft (grant no GU360/15-1 to AHG; FL 377/2-1 and FOR1336 to AF) and by the Wellcome Trust (Biomedical Research Collaboration Grant 068065 to BVLP and AHG).

## REFERENCES

- Aarhus, R., Graeff, R. M., Dickey, D. M., Walseth, T. F., and Lee, H. C. (1995). ADP-ribosyl cyclase and CD38 catalyze the synthesis of a calcium-mobilizing metabolite from NADP. *J. Biol. Chem.* 270, 30327–30333.
- Badour, K., Zhang, J., Shi, F., McGavin, M. K., Rampersad, V., Hardy, L. A., Field, D., and Siminovich, K. A. (2003). The Wiskott-Aldrich syndrome protein acts downstream of CD2 and the CD2AP and PSTPIP1 adaptors to promote formation of the immunological synapse. *Immunity* 18, 141–154.
- Barceló-Torns, M., Lewis, A. M., Gubern, A., Barneda, D., Bloor-Young, D., Picatoste, F., Churchill, G. C., Claro, E., and Masgrau, R. (2011). NAADP mediates ATP-induced Ca<sup>2+</sup> signals in astrocytes. *FEBS Lett.* 585, 2300–2306.
- Berg, I., Potter, B. V., Mayr, G. W., and Guse, A. H. (2000). Nicotinic acid adenine dinucleotide phosphate (NAADP+) is an essential regulator of T-lymphocyte Ca<sup>2+</sup>-signaling. *J. Cell Biol.* 150, 581–8.
- Brailoiu, E., Churamani, D., Cai, X., Schrlau, M. G., Brailoiu, G. C., Gao, X., Hooper, R., Boulware, M. J., Dun, N. J., Marchant, J. S., and Patel, S. (2009). Essential requirement for two-pore channel 1 in NAADP-mediated calcium signaling. *J. Cell Biol.* 186, 201–209.
- Calcraft, P. J., Ruas, M., Pan, Z., Cheng, X., Arredouani, A., Hao, X., Tang, J., Rietdorf, K., Teboul, L., Chuang, K. T., Lin, P., Xiao, R., Wang, C., Zhu, Y., Lin, Y., Wyatt, C. N., Parrington, J., Ma, J., Evans, A. M., Galione, A., and Zhu, M. X. (2009). NAADP mobilizes calcium from acidic organelles through two-pore channels. *Nature* 459, 596–600.
- Cordiglieri, C., Odoardi, F., Zhang, B., Nebel, M., Kawakami, N., Klinkert, W. E., Lodygin, D., Lühder, F., Breunig, E., Schild, D., Ulaganathan, V. K., Dornmair, K., Dammermann, W., Potter, B. V., Guse, A. H., and Flügel, A. (2010). Nicotinic acid adenine dinucleotide phosphate-mediated calcium signalling in effector T cells regulates autoimmunity of the central nervous system. *Brain* 133, 1930–1943.
- Cosker, F., Cheviron, N., Yamasaki, M., Menteyne, A., Lund, F. E., Moutin, M. J., Galione, A., and Cancela, J. M. (2010). The ecto-enzyme CD38 is a nicotinic acid adenine dinucleotide phosphate (NAADP) synthase that couples receptor activation to Ca<sup>2+</sup> mobilization from lysosomes in pancreatic acinar cells. *J. Biol. Chem.* 285, 38251–38259.
- Dammermann, W. and Guse, A. H. (2005). Functional ryanodine receptor expression is required for NAADP-mediated local Ca<sup>2+</sup> signaling in T-lymphocytes. *J. Biol. Chem.* 280, 21394–21399.
- Dammermann, W., Zhang, B., Nebel, M., Cordiglieri, C., Odoardi, F., Kirchberger, T., Kawakami, N., Dowden, J., Schmid, F., Dornmair, K., Hohenegger, M., Flügel, A., Guse, A. H., and Potter, B. V. L. (2009). NAADP-mediated Ca<sup>2+</sup> signaling via type 1 ryanodine receptor in T cells revealed by a synthetic NAADP antagonist. *Proc. Natl. Acad. Sci. U.S.A.* 106, 10678–83.
- Davis, L. C., Morgan, A. J., Chen, J. L., Snead, C. M., Bloor-Young, D., Shenderov, E., Stanton-Humphreys, M. N., Conway, S. J., Churchill, G. C., Parrington, J., Cerundolo, V., and Galione, A. (2012). NAADP Activates Two-Pore Channels on T Cell Cytolytic Granules to Stimulate Exocytosis and Killing. *Curr. Biol.* doi:pii: S0960-9822(12)01256-0.10.1016/j.cub.2012.10.035. [Epub ahead of print]
- Donnadieu, E., Bismuth, G., and Trautmann, A. (1994). Antigen recognition by helper T cells elicits a sequence of distinct changes of their shape and intracellular calcium. *Curr. Biol.* 4, 584–595.
- Eylar, E. H., Jackson, J. J., and Kniskern, P. J. (1979). Suppression and reversal of allergic encephalomyelitis in rhesus monkeys with basic protein and peptides. *Neurochem. Res.* 4, 249–58.
- Flügel, A., Willem, M., Berkowicz, T., and Wekerle, H. (1999). Gene transfer into CD4+ T lymphocytes: Green fluorescent protein-engineered, encephalitogenic T cells illuminate brain autoimmune responses. *Nat. Med.* 5, 843–7.
- Gasser, A., Bruhn, S., and Guse, A. H. (2006). Second messenger function of nicotinic acid adenine dinucleotide phosphate revealed by an improved enzymatic cycling assay. *J. Biol. Chem.* 281, 16906–13.
- Gerasimenko, J. V., Maruyama, Y., Yano, K., Dolman, N. J., Tepikin, A. V., Petersen, O. H., and Gerasimenko, O. V. (2003). NAADP mobilizes Ca<sup>2+</sup> from a thapsigargin-sensitive store in the nuclear envelope by activating ryanodine receptors. *J. Cell Biol.* 163, 271–82.
- Gerasimenko, J. V., Sherwood, M., Tepikin, A. V., Petersen, O. H., and Gerasimenko, O. V. (2006). NAADP, cADPR and IP<sub>3</sub> all release Ca<sup>2+</sup> from the endoplasmic reticulum and an acidic store in the secretory granule area. *J. Cell. Sci.* 119, 226–38.
- Guse, A. H., Goldwisch, A., Weber, K., and Mayr, G. W. (1995). Non-radioactive, isomer-specific inositol phosphate mass determinations: high-performance liquid chromatography-micro-metal-dye detection strongly improves speed and sensitivity of analyses from cells and micro-enzyme assays. *J. Chromatogr. B Biomed. Appl.* 672, 189–198.
- Guse, A. H. (2012). Linking NAADP to ion channel activity: A unifying hypothesis. *Sci. Signal.* 5, pe18.
- Guse, A. H. and Lee, H. C. (2008). NAADP: a universal Ca<sup>2+</sup> trigger. *Sci Signal* 1, re10.
- Guse, A. H., Roth, E., and Emmrich, F. (1993). Intracellular Ca<sup>2+</sup> pools in Jurkat T-lymphocytes. *Biochem. J.* 291, 447–51.
- Guse, A. H., da Silva, C. P., Berg, I., Skapenko, A. L., Weber, K., Heyer, P., Hohenegger, M., Ashamu, G. A., Schulze-Koops, H., Potter, B. V., and Mayr, G. W. (1999). Regulation of calcium signalling in T lymphocytes by the second messenger cyclic ADP-ribose. *Nature* 398, 70–73.
- Hohenegger, M., Suko, J., Gscheidlinger, R., Drobny, H., and Zidar, A. (2002). Nicotinic acid-adenine dinucleotide phosphate activates the skeletal muscle ryanodine receptor. *Biochem. J.* 367, 423–431.
- Kaizuka, Y., Douglass, A. D., Varma, R., Dustin, M. L., and Vale, R. D. (2007). Mechanisms for segregating T cell receptor and adhesion molecules during immunological synapse formation in Jurkat T cells. *Proc. Natl. Acad. Sci. USA.* 104, 20296–20301.
- Kim, B., Park, K., Yim, C., Takasawa, S., Okamoto, H., Im, M., and Kim, U. (2008). Generation of nicotinic acid adenine dinucleotide phosphate and cyclic ADP-ribose by glucagon-like peptide-1 evokes Ca<sup>2+</sup> signal that is essential for insulin secretion in mouse pancreatic islets. *Diabetes* 57, 868–78.
- Krummel, M. F. and Cahalan, M. D. (2010). The immunological synapse: A dynamic platform for local signaling. *J. Clin. Immunol.* 30, 364–372.
- Kunerth, S., Mayr, G. W., Koch-Nolte, F., and Guse, A. H. (2003). Analysis of subcellular calcium signals in T-lymphocytes. *Cell. Signal.* 15, 783–92.



- Kunerth, S., Langhorst, M. F., Schwarzmann, N., Gu, X., Huang, L., Yang, Z., Zhang, L., Mills, S. J., Zhang, L., Potter, B. V. L., and Guse, A. H. (2004). Amplification and propagation of pacemaker  $\text{Ca}^{2+}$  signals by cyclic ADP-ribose and the type 3 ryanodine receptor in T cells. *J. Cell. Sci.* 117, 2141–2149.
- Langhorst, M. F., Schwarzmann, N., and Guse, A. H. (2004).  $\text{Ca}^{2+}$  release via ryanodine receptors and  $\text{Ca}^{2+}$  entry: Major mechanisms in NAADP-mediated  $\text{Ca}^{2+}$  signaling in T-lymphocytes. *Cell. Signal.* 16, 1283–9.
- Lee, H. C. (2012). Cyclic ADP-ribose and nicotinic acid adenine dinucleotide phosphate (NAADP) as messengers for calcium mobilization. *J. Biol. Chem.* 287, 31633–31640.
- Lee, H. C. (2012). The cyclic ADP-Ribose/NAADP/CD38-signaling pathway: Past and present. *Messenger* 1, 16–33.
- Lee, H. C. and Aarhus, R. (1995). A derivative of NADP mobilizes calcium stores insensitive to inositol trisphosphate and cyclic ADP-ribose. *J. Biol. Chem.* 270, 2152–2157.
- Lewis, A. M., Aley, P. K., Roomi, A., Thomas, J. M., Masgrau, R., Garnham, C., Shipman, K., Paramore, C., Bloor-Young, D., Sanders, L. E., Terrar, D. A., Galione, A., and Churchill, G. C. (2012).  $\beta$ -Adrenergic receptor signaling increases NAADP and cADPR levels in the heart. *Biochem. Biophys. Res. Commun.* 427, 326–329.
- Lin-Moshier, Y., Walseth, T. F., Churamani, D., Davidson, S. M., Slama, J. T., Hooper, R., Brailoiu, E., Patel, S., and Marchant, J. S. (2012). Photoaffinity labeling of nicotinic acid adenine dinucleotide phosphate (NAADP) targets in mammalian cells. *J. Biol. Chem.* 287, 2296–2307.
- Masgrau, R., Churchill, G. C., Morgan, A. J., Ashcroft, S. J., and Galione, A. (2003). NAADP: a new second messenger for glucose-induced  $\text{Ca}^{2+}$  responses in clonal pancreatic beta cells. *Curr. Biol.* 13, 247–251.
- Mojzisoová, A., Krizanová, O., Záciková, L., Komínková, V., and Ondrias, K. (2001). Effect of nicotinic acid adenine dinucleotide phosphate on ryanodine calcium release channel in heart. *Pflugers Arch.* 441, 674–677.
- Morgan, A. J., Platt, F. M., Lloyd-Evans, E., and Galione, A. (2011). Molecular mechanisms of endolysosomal  $\text{Ca}^{2+}$  signalling in health and disease. *Biochem. J.* 439, 349–374.
- Nolz, J. C., Gomez, T. S., Zhu, P., Li, S., Medeiros, R. B., Shimizu, Y., Burkhardt, J. K., Freedman, B. D., and Billadeau, D. D. (2006). The WAVE2 complex regulates actin cytoskeletal reorganization and CRAC-mediated calcium entry during T cell activation. *Curr. Biol.* 16, 24–34.
- Ogunbayo, O. A., Zhu, Y., Rossi, D., Sorrentino, V., Ma, J., Zhu, M. X., and Evans, A. M. (2011). Cyclic adenosine diphosphate ribose activates ryanodine receptors, whereas NAADP activates two-pore domain channels. *J. Biol. Chem.* 286, 9136–9140.
- Schmid, F., Bruhn, S., Weber, K., Mittrücker, H. W., and Guse, A. H. (2011). CD38: A NAADP degrading enzyme. *FEBS Lett.* 585, 3544–3548.
- Soares, S., Thompson, M., White, T., Isbell, A., Yamasaki, M., Prakash, Y., Lund, F. E., Galione, A., and Chini, E. N. (2007). NAADP as a second messenger: Neither CD38 nor base-exchange reaction are necessary for in vivo generation of NAADP in myometrial cells. *Am. J. Physiol. Cell. Physiol.* 292, C227–239.
- Steen, M., Kirchberger, T., and Guse, A. H. (2007). NAADP mobilizes calcium from the endoplasmic reticular  $\text{Ca}^{2+}$  store in T-lymphocytes. *J. Biol. Chem.* 282, 18864–71.
- Walseth, T. F., Lin-Moshier, Y., Weber, K., Marchant, J. S., Slama, J. T., and Guse, A. H. (2012). Nicotinic acid adenine dinucleotide 2'-phosphate (NAADP) binding proteins in T-lymphocytes. *Messenger* 1, 86–94.
- Wang, X., Zhang, X., Dong, X. P., Samie, M., Li, X., Cheng, X., Goschka, A., Shen, D., Zhou, Y., Harlow, J., Zhu, M. X., Clapham, D. E., Ren, D., and Xu, H. (2012). TPC proteins are phosphoinositide-activated sodium-selective ion channels in endosomes and lysosomes. *Cell* 151, 372–383.
- Yamaguchi, S., Jha, A., Li, Q., Soyombo, A. A., Dickinson, G. D., Churamani, D., Brailoiu, E., Patel, S., and Muallem, S. (2011). Transient receptor potential mucolipin 1 (TRPML1) and two-pore channels are functionally independent organellar ion channels. *J. Biol. Chem.* 286, 22934–22942.
- Yamasaki, M., Thomas, J. M., Churchill, G. C., Garnham, C., Lewis, A. M., Cancela, J. M., Patel, S., and Galione, A. (2005). Role of NAADP and cADPR in the induction and maintenance of agonist-evoked  $\text{Ca}^{2+}$  spiking in mouse pancreatic acinar cells. *Curr. Biol.* 15, 874–878.
- Zhang, F. and Li, P. (2007). Reconstitution and characterization of a nicotinic acid adenine dinucleotide phosphate (NAADP)-sensitive  $\text{Ca}^{2+}$  release channel from liver lysosomes of rats. *J. Biol. Chem.* 282, 25259–69.
- Zhang, F., Jin, S., Yi, F., and Li, P. (2009). TRP-ML1 functions as a lysosomal NAADP-sensitive  $\text{Ca}^{2+}$  release channel in coronary arterial myocytes. *J. Cell. Mol. Med.* 13, 3174–85.

Received: 1 October 2014. Accepted: 20 October 2015.